Journal of Power Sources 257 (2014) 192–197

Contents lists available at ScienceDirect

Journal of Power Sources

journal homepage: www.elsevier.com/locate/jpowsour

Hybrid network CuS monolith cathode materials synthesized via facile *in situ* melt-diffusion for Li-ion batteries

Juanjuan Cheng, Yong Pan*, Jingtao Zhu, Zhenzhen Li, Junan Pan, Zengsheng Ma*

Key Laboratory of Low Dimensional Materials and Application Technology of Ministry of Education, and Faculty of Materials, Optoelectronics and Physics, Xiangtan University, Xiangtan 411105, Hunan, China

HIGHLIGHTS

- 3D hybrid network CuS monolith cathode for Li-ion batteries.
- Initial capacity of 185.1 mAh g^{-1} and increasing capacity with cycle number.
- Excellent cycle ability with capacity of 468.3 mAh g^{-1} retention after 100 cycles.
- Stepwise utilization of active material keeps increase of capacity.

ARTICLE INFO

Article history:
Received 12 October 2013
Received in revised form
17 January 2014
Accepted 28 January 2014
Available online 8 February 2014

Keywords:
CuS cathode
Binder-free
Hybrid network
Li-ion battery

ABSTRACT

A hybrid network CuS monolith cathode, consisting of the microporous network formed by CuS sheets and particles on three-dimensional macroporous monolith Cu foam, is synthesized by a facile *in situ* melt-diffusion strategy without binder for Li-ion batteries. The cathode shows an abnormal capacity of 185.1 and 468.3 mAh g^{-1} CuS for the first and 100th cycle at a current rate of 0.2 C (1 C = 560 mA g^{-1}), respectively. And it could recover 83.9% of the capacity after cycled at various current rates, demonstrating an excellent rate capability which outperforms many other currently available CuS cathodes.

1. Introduction

There has been a rapid development in portable electronics, hybrid electric vehicles (HEV), electric vehicles (EV) and large-scale smart grids, which in turn requires rechargeable batteries with high energy and high power densities as a power source [1–3]. Unfortunately, further applications of the commercialized batteries are limited because of their low energy and power densities, which are restricted to the theoretical specific capacities of the anode and cathode materials [4–6]. For example, the theoretical specific capacities of cathode materials based on lithium transition metal oxide or phosphates are between 150 and 200 mAh g^{-1}. It is more urgently needed to develop new cathode materials to achieve higher energy storage for the lithium ion batteries [7].

Sulfur and sulfur composites are attractive cathodes with high theoretical specific capacities [8–10]. Copper sulfide (CuS) exhibits a moderate theoretical specific capacity (560 mAh g^{-1}) and a good electrical conductivity (10^{-3} S cm^{-1}) compared with 1675 mAh g^{-1} and 5×10^{-30} S cm^{-1} of sulfur. Hence, CuS is potential for higher active materials utilization and higher coulombic efficiency [11–13]. Though many CuS cathodes have been investigated [14–16], the Li/CuS batteries still cannot be commercialized due to poor cycle life, low active material utilization, and low charge efficiency, which are related to the dissolution of lithium polysulfides formed during discharge. Additionally, few attentions have been paid to the volumetric change of CuS during lithiation process, which leads to the material pulverization and the reduction of electrochemical cycle life [17]. At the same time, the synthesis processes of CuS materials are very complex and binders and conductive additives are requisite to prepare electrode [18,19].

Designing special architectures is one of the most promising routes to solve the degeneration problem for many electrodes. For example, Cu foam has been successfully employed in Ge and Sn

* Corresponding authors. Key Laboratory of Low Dimensional Materials & Application Technology, Xiangtan University, Hunan 411105, China. Tel./fax: +86 731 58293577.
E-mail addresses: ypan@xtu.edu.cn (Y. Pan), zsma@xtu.edu.cn (Z. Ma).

http://dx.doi.org/10.1016/j.jpowsour.2014.01.124
0378-7753/

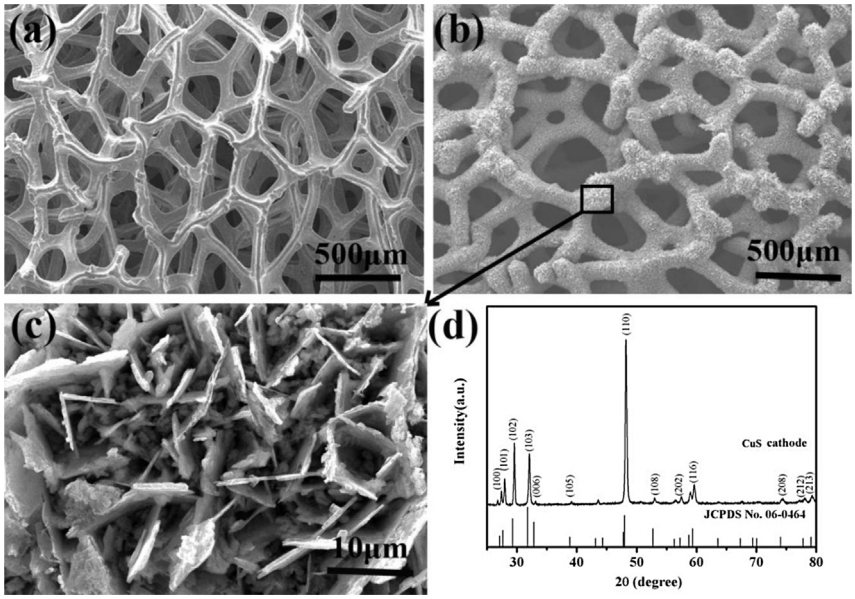

Fig. 1. Characterization of the Cu foam and the obtained hybrid network CuS monolith cathode. (a) SEM image of Cu foam; (b) low-magnification SEM image of CuS; (c) high-magnification SEM image of CuS and (d) XRD pattern of CuS cathode.

anodes which exhibit enhanced electrochemical performance [20–22]. It is because three-dimensional (3D) electrodes with interconnected porous networks are beneficial to improve the utilization of active materials, facilitate the immersion of electrolyte, and provide a short diffusion path of ions. Furthermore, yolk-shell and hollow spheres structures with spare space have been designed in sulfur and V_2O_5 cathode to accommodate the volumetric changes and thus to improve the cycle performance [23–25].

In this paper, we report a hybrid network CuS monolith cathode using a facile *in situ* melt-diffusion method without binders and conductive additives. The cathode is constructed by the microporous network with spare space formed by CuS sheets and particles on 3D macroporous monolith Cu foam. The electrochemical performances of the CuS cathode are enhanced simultaneously.

2. Experimental

2.1. Preparation of CuS electrodes

A typical procedure for the synthesis of the hybrid network CuS monolith cathode is shown as follow. Firstly, the Cu foam (90 pores per inch, 650 g m^{-2} surface density, and about 2.5 mm thick) was cut into pieces of 1 cm × 1 cm and cleaned with ultrasonic for 5 min in 1 M HCl solution and in deionized water, respectively. Secondly, the samples were dried in vacuum at 60 °C for 6 h. Thirdly, sulfur (99.99%) was ground for 30 min, and then sprinkled into the dried Cu foam homogeneously. The weight ratio of sulfur:Cu foam was about 1:2 being consistent to the composition of CuS. Fourthly, the Cu foam covered with sulfur was encapsulated in the ceramic boat and heated in a furnace at 155 °C for 3 h in the argon protection environment. Finally, the samples were cooled naturally to room temperature and weighed. The experiments showed that the sulfur loading was about 3 mg on per Cu foam piece, and the CuS active material was 9 mg on per electrode piece assuming that all sulfur remained on the Cu foam combined into CuS.

2.2. Structural characterization

The surface morphologies and microstructures of the CuS cathode before and after cycles were characterized by scanning electron microscopy (SEM, Hitachi S-4800) and X-ray diffraction (XRD, Rigaku D/Max-2400) with Cu K_α radiation ($\lambda = 0.1542$ nm).

2.3. Electrochemical measurements

The coin-type 2025 cells consisting of the obtained CuS cathode, a metallic lithium anode, and a Celgard separator were assembled in an argon-filled glovebox. The electrolyte was 1 M lithium bis (trifluoromethanesulfonyl) imide (LiTFSI) dissolved in a 1:1 volume ratio mixture of 1,3-dioxolane and dimethoxy ethane.

All the electrochemical measurements were carried out at room temperature. Electrochemical discharge/charge and cycle performance, under the potential window 3.0–1.0 V vs. Li/Li^+, were conducted using Battery Test System (Neware, Shenzhen, China). Cyclic voltammetry (CV) and electrochemical impedance spectroscopy (EIS) studies were measured by a CHI660D Electrochemical Workstation (Chenhua, Shanghai, China).

3. Results and discussion

The SEM images of hybrid network CuS monolith cathode are presented in Fig. 1. In the panoramic view of the CuS (Fig. 1b), it can be clearly seen that CuS cathode has many macropores in the range of 500 μm to 1 mm, which completely retains the porous and 3D interconnected network structure of the Cu foam (Fig. 1a). The CuS was directly nucleated on the skeleton providing a strong bonding between CuS and Cu and it is composed of plenty of sheets and particles in Fig. 1c. The sheets with several hundred nanometers in thickness and 10 μm in width stand face to face perpendicular to the substrate. The growth mechanism of CuS sheets and particles may be the combination of copper ion with the sulfide ion into CuS on the surface of the crystal along the preferential direction of the copper foam [26,27]. Between the sheets and particles, spare spaces can be seen. And the microporous network of CuS sheets and particles was formed on 3D macroporous monolith Cu foam, viz., the hybrid network CuS monolith cathode. This cathode promises efficient electrolyte immersion and shortens the ion diffusion length, which makes rapid Li ion and charge transformation [21].

Fig. 1d shows the XRD pattern of the hybrid network CuS monolith cathode before cycling. All the diffraction peaks of the

sample can be indexed with the hexagonal phase of CuS (JCPDS No. 06-0464), and no other peaks of impurities were detected, indicating a synthesized pure CuS cathode materials on Cu foam. The main reason may be that Cu could react with sulfur fully when sulfur was heated to be of lowest viscosity during the preparation process [8]. Additionally, the (110) peaks showed much higher intensity contrasting to the standard powder, which demonstrates certain preferential orientation.

The galvanostatic discharge/charge curves of the hybrid network CuS monolith cathode in the first 100 cycles at a current rate of 0.2 C (1 C = 560 mA g^{-1}) are shown in Fig. 2. In the discharge curve, it clearly shows two plateaus at 2.05 V and 1.68 V, indicating the Li ion intercalation into CuS lattices to form Li_2S and Cu [16]. In the first 20 cycles (Fig. 2a), it can be seen clearly that the plateau of 2.05 V shortens to disappear with cycle number, while the lower voltage plateau of 1.68 V becomes longer. In the 30–100 cycles (Fig. 2b), the higher voltage plateaus appear again at the 60th cycle, and it is about 2.2 V which is higher than the corresponding plateau in the first 20 cycles of 2.05 V. In the charge curve, the similar change trend of the corresponding charge plateau and reaction was also found. The changes of the discharge/charge curves will be clarified combining with the CV data and cycle performance later.

Fig. 3a shows the first four cycles CV curves of the CuS cathode conducted at a sweep rate of 0.2 mV s^{-1} in the voltage range of 1.2–3.0 V vs Li/Li^+. Typical characteristics for electrochemical reactions between CuS and Li ions have been observed by the cathodic and anodic peaks. At the first cycle, the cathodic peak at 2.05 V is related

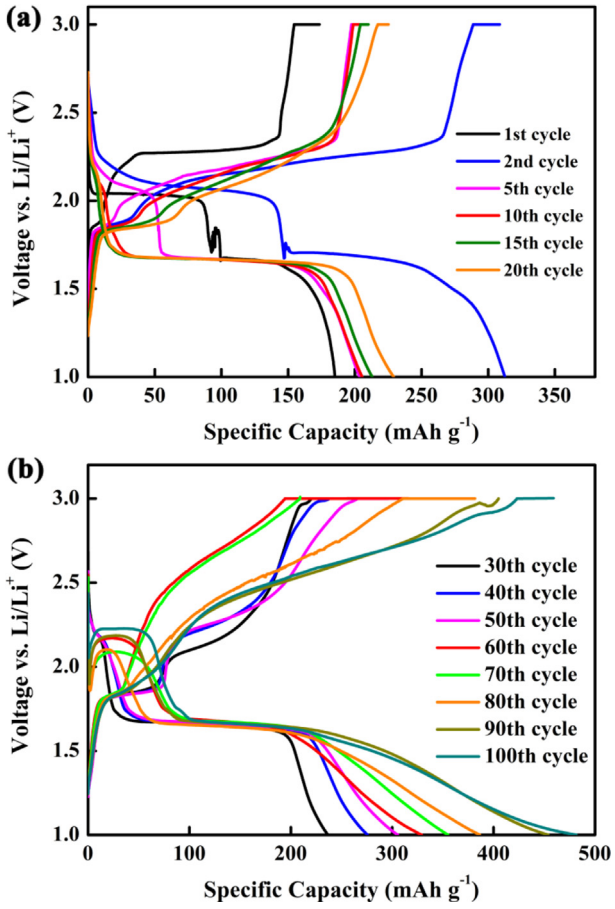

Fig. 2. The discharge/charge curves of the hybrid network CuS monolith cathode with cycling at a current rate of 0.2 C (1 C = 560 mA g^{-1}). (a) Discharge/charge curves for the 1st–20th cycles; (b) discharge/charge curves for the 30th–100th cycles.

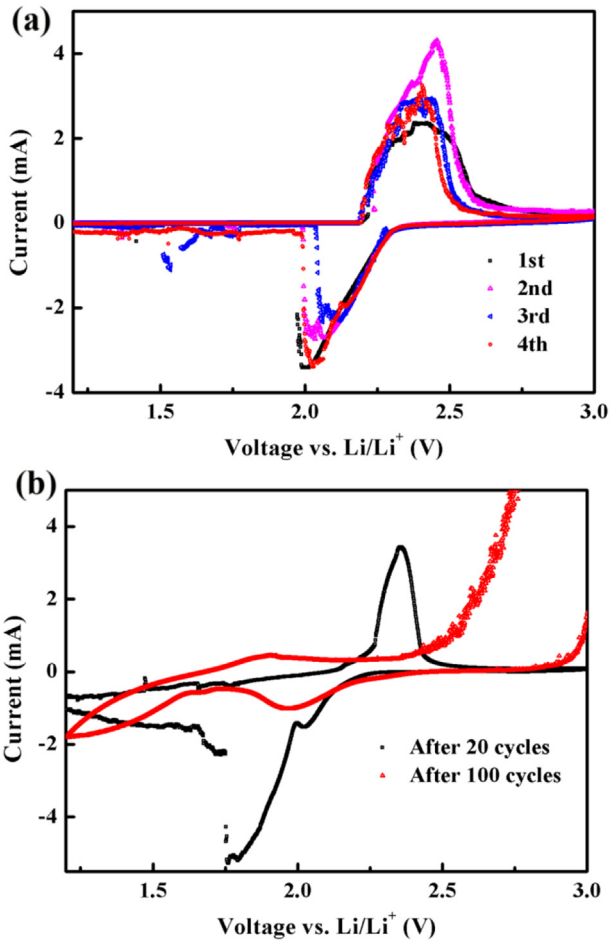

Fig. 3. CV curves of the hybrid network CuS monolith cathode (collected at a sweep rate of 0.2 mV s^{-1} in the voltage range of 1.2–3.0 V vs Li/Li^+). (a) CV before cycling; (b) CV after 20 and 100 discharge/charge cycles at a current rate of 0.2 C (1 C = 560 mA g^{-1}).

to the formation of Li_xCuS, and the following peak at about 1.6 V is associated with further chemical reaction to Li_2S and Cu [11], exhibiting a consistency with the discharge plateaus in Fig. 2. In the subsequent anodic scan, only an anodic peak appears at 2.25–2.4 V related to the complete conversion into CuS, and the high potential value is attributed to the polarization during the conversion into CuS [28]. At the second cycle, the anodic peak currents increase obviously, while the cathodic peak currents decrease slightly, indicating the formation and the migration of lithium polysulfides [29]. At the third and fourth cycles, encouragingly, the cathodic peak positions is shifted to slightly higher potentials and anodic peak positions to lower potentials, suggesting improvement of electrochemical cycle reversibility. In order to further explore the change of electrochemical reaction for the CuS cathode, the CV data at 20 and 100 cycles were collected, respectively, as shown in Fig. 3b. It can be seen that the cathodic and anodic peaks after 20 discharge/charge cycles are similar to these at the first four cycles. After 100 cycles, the cathodic and anodic peaks positions are at 2.0 V and 1.8 V respectively, demonstrating the appearance of the charge and discharge potential plateaus at the 60th cycle shown in Fig. 2b. But the peaks become weaker and broader. The remarkable broad peak among 2.5–2.7 V may be attributed to the lithium polysulfides dissolution.

The long term cycling performances of the hybrid network CuS monolith cathode are shown in Fig. 4. From Fig. 4a, it can be seen

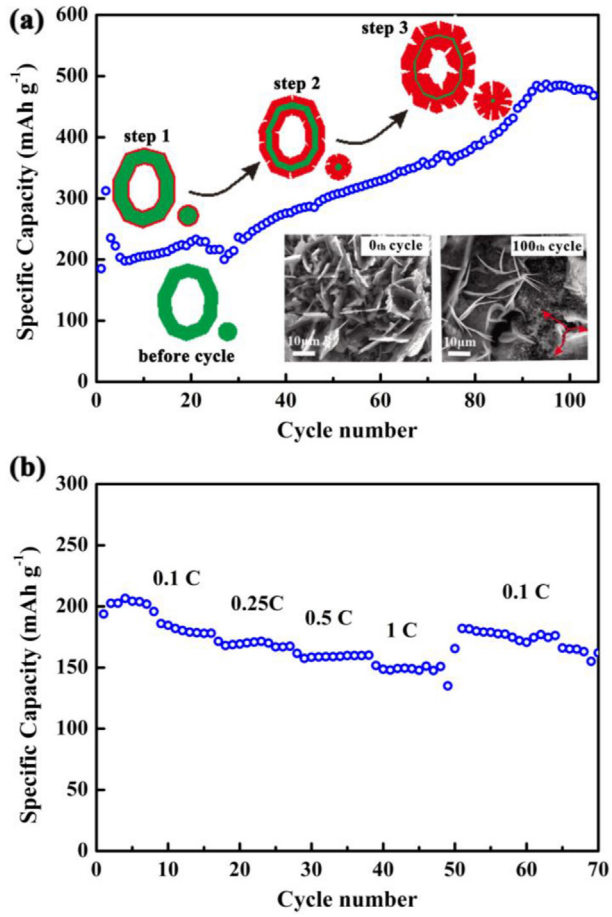

Fig. 4. Cycle performance and rate capability of the hybrid network CuS monolith cathode. (a) Cycle life at a current rate of 0.2 C (1 C = 560 mA g^{-1}), along with a proposed schematic diagram of CuS cathode for improving capacity (insert: SEM images of the CuS cathode before and after 100 cycles); (b) rate capability at various current rates gradually increased from 0.1 C to 1 C and reduced back to 0.1 C.

that an initial discharge capacity of 185.1 mAh g^{-1} at a current rate of 0.2 C is obtained, which is about one third of the theoretical capacity of CuS (560 mAh g^{-1}). It may derive from the incomplete activation of the core CuS active material enveloped by the shell CuS in the hybrid network. The capacity increases in the second cycle and fades from the third to sixth cycle. The fating is mainly due to the formation of Li_2S which is insulating and has poor reversibility [30]. After six cycles, the CuS cathode delivers an increasing reversible capacity with cycle number. After 100 cycles, a stable capacity of 468.3 mAh g^{-1} is obtained, which is 2.5 times higher than the initial value, inspiring that more active material CuS is involved in the electrochemical process [30,31]. The SEM image (inset of Fig. 4a) of CuS cathode after 100 cycles shows gaps with the width of 2–3 μm and the length of about 10 μm, which exposes fresh CuS, soaks more electrolyte and helps the diffusion of Li^+. Combining with the appearance of the higher discharge plateaus again at 60th–100th discharge/charge curves in Fig. 2b, it can be deduced that the increase of capacity with the cycle number is due to more fresh CuS exposed through gaps introduced by expansion of CuS gradually. From the results of discharge/charge, CV curves, SEM images and cycle performances of the hybrid network CuS monolith cathode whose schematic diagram for improving capacity is constructed in Fig. 4a. In step 1, the electrochemical red-ox reactions take place between Li^+ and CuS on the skeleton surface, and partial Li_2S cannot recover to CuS, which is verified by the shortening of the higher discharge plateau in Fig. 2. In steps 2 and 3, the gaps among the skeleton occur due to the expansion of the CuS with cycling, exposing fresh CuS to join in electrochemical process. At the same time, the lithium polysulfides concentration in the electrolyte increases with the cycle number, and thus the concentration gradient between electrolyte and the cathode decreases gradually, which slows down the dissolution of lithium polysulfides, facilitating improvement of cycle performance and utilization of active material [32]. We believe that the stepwise utilization of active material and a reduced dissolution of polysulfides promise the increase of the capacity and cycle life [33,34]. Unlike other CuS electrodes, the hybrid network CuS monolith cathode reported in this paper is interweaved by sheets and particles on 3D macroporous monolith Cu foam, whose hybrid network constructs a cavity to constraint polysulfides and provide a spare space for the charging expansion of the active materials. Furthermore, due to the easier soak of the electrolyte and larger electrode surface area, the CuS cathode possesses short solid-state ion diffusion length and fast electron transfer. Actually, the excellent rate capability shows that a 83.9% capacity retention can be obtained after 70 cycles at rates from 0.1 to 1 C and then back to 0.1 C, as shown in Fig. 4b.

The superior cycle performance and rate capability of the hybrid network CuS monolith cathode is illustrated from the charge-transfer kinetics by the electrochemical impedance spectroscopy (EIS) in Fig. 5. The semicircle in the high frequency region corresponds to the charge-transfer resistance of the electrolyte–electrode interface [35,36]. The charge-transfer resistance values are195.5 and 25.7 Ω for before and after 100 cycles, respectively, indicating an improved conductivity of the electrode and a better wetting of the electrolyte through the electrode due to the hybrid network structure. However, the electrolyte resistance corresponding to the intersection between the high frequency semicircle and the real axis increases slightly after 100 cycles due to the enhancement of the electrolyte viscosity. This indicates that partly dissolution of polysulfides agrees well with the CV results after 100 cycles in Fig. 3b.

The interface reaction is related to the cycle performance and rate capability owing to the precipitation of insoluble Li_2S. The phase structure and morphology of the hybrid network CuS monolith cathode in the fully charged state after 100 cycles at a current rate of 0.2 C were studied by XRD and SEM to reveal the

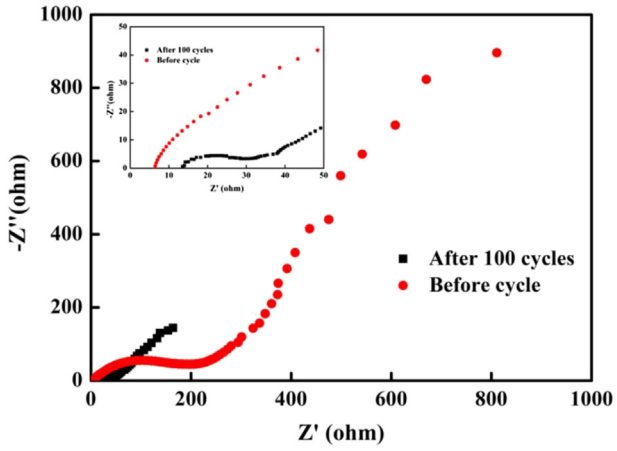

Fig. 5. EIS patterns of the hybrid network CuS monolith cathode before and after 100 discharge/charge cycles at a current rate of 0.2 C (1 C = 560 mA g^{-1}) fully charging to 3 V (insert: the magnified spectrum in the high frequency region); the EIS measurements were performed in the frequency range of 1 MHz to 0.1 Hz with an AC voltage amplitude of 5 mV at the open-circuit voltage.

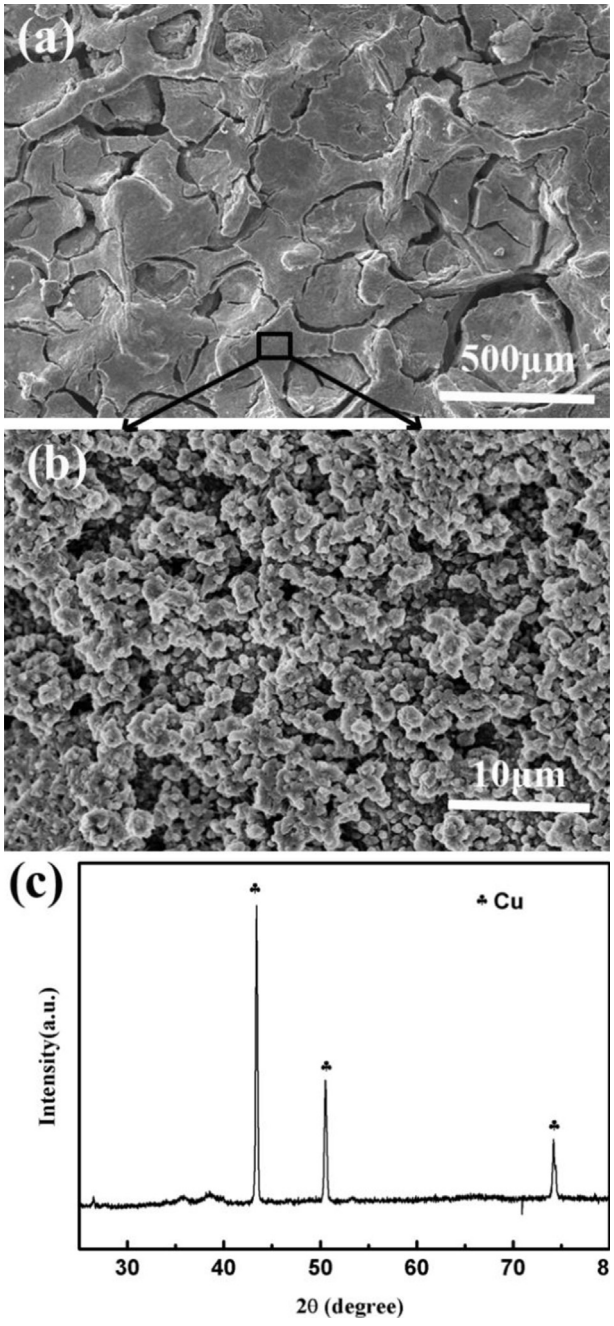

Fig. 6. SEM images and XRD pattern of the hybrid network CuS monolith cathode cycled after 100 times at a current rate of 0.2 C (1 C = 560 mA g^{-1}). (a) Low-magnification SEM image; (b) high-magnification SEM image; (c) XRD pattern.

interface reaction. The results are shown in Fig. 6. The detailed processes are following. Firstly, carefully take out of the cathode from the coin cell in the argon-filled glovebox. Secondly, wash it with 1,3-dioxolane (DOL) solution. Lastly, dry it in vacuum. In Fig. 6a and b, it can be seen that the morphology of the cycled cathode is much different from the obtained CuS cathode (Fig. 2b and c). The macroporous of the cycled one is filled by the precipitation of insoluble products and the CuS sheets change to round particles due to the expansion of the cathode. It is noted that the cycled CuS cathode is porous formed by the interconnected round particles, being easy to the reactions between the electrolyte and electrode [37,38], which could be evidenced from the EIS pattern shown in Fig. 5. In Fig. 6c, the strong diffraction peaks corresponding to Cu is detected in the XRD pattern, which is due to the dissolution of the CuS on the electrode surface during cycling as well as the exposure of Cu substrate. The porous architecture combining with the high conductivity of the exposed Cu provides the decreased charge-transfer resistance. Thus, the gradually increased capacity and the improved cycle performance are obtained.

4. Conclusions

In summary, a hybrid network CuS monolith cathode without binder has been fabricated by a facile and low-cost method. There is an outstanding cycling performance of the cathode with an initial capacity of 185.1 mAh g^{-1} and a reversible capacity of 468.3 mAh g^{-1} after 100 cycles at a current rate of 0.2 C. An excellent rate capability of 83.9% capacity recovery is also obtained at various current rates. The microporous and 3D macroporous hybrid network monolith structures have been proven to improve the cycle performance and rate capability of the cathode. We believe that the binder-free CuS cathode with unique architecture is potential for high life and power rechargeable batteries.

Acknowledgments

This work was supported by the National Natural Science Foundation of China (Nos. 11372267 and 11102176), the Emerging Strategic Industries of Hunan Province (2012GK4075), the Science and Technology Program of Hunan Province (2013GK3163) and the Graduate Innovation Program of Hunan Province (CX2013B258)

References

[1] M. Armand, J.M. Tarascon, Nature 451 (2008) 652–657.
[2] F. Cheng, J. Liang, Z. Tao, J. Chen, Adv. Mater. 23 (2011) 1695–1715.
[3] J.M. Tarascon, M. Armand, Nature 414 (2001) 359–367.
[4] M.S. Whittingham, Chem. Rev. 104 (2004) 4271–4302.
[5] A. Manthiram, J. Phys. Chem. Lett. 2 (2011) 176–184.
[6] B.L. Ellis, K.T. Lee, L.F. Nazar, Chem. Mater. 22 (2010) 691–714.
[7] K. Kang, Y.S. Meng, J. Breger, C.P. Grey, G. Ceder, Science 311 (2006) 977–980.
[8] X. Ji, K.T. Lee, L.F. Nazar, Nat. Mater. 8 (2009) 500–506.
[9] H. Kim, J.T. Lee, G. Yushin, J. Power Sources 226 (2013) 256–265.
[10] X. Liang, Z. Wen, Y. Liu, H. Zhang, J. Jin, M. Wu, X. Wu, J. Power Sources 206 (2012) 409–413.
[11] Y. Wang, X. Zhang, P. Chen, H. Liao, S. Cheng, Electrochim. Acta 80 (2012) 264–268.
[12] Y. Chen, C. Davoisne, J.M. Tarascon, C. Guery, J. Mater. Chem. 22 (2012) 5295–5299.
[13] J.S. Kim, D.Y. Kim, G.B. Cho, T.H. Nam, K.W. Kim, H.S. Ryu, J.H. Ahn, H.J. Ahn, J. Power Sources 189 (2009) 864–868.
[14] C.H. Lai, K.W. Huang, J.H. Cheng, C.Y. Lee, B.J. Hwang, L.J. Chen, J. Mater. Chem. 20 (2010) 6638–6645.
[15] Q. Li, Y. Xue, Y. Zhu, Y. Qian, J. Nanosci. Nanotechnol. 13 (2013) 1265–1269.
[16] J.S. Chung, H.J. Sohn, J. Power Sources 108 (2002) 226–231.
[17] X. He, J. Ren, L. Wang, W. Pu, C. Jiang, C. Wan, J. Power Sources 190 (2009) 154–156.
[18] A. Hayashi, T. Ohtomo, F. Mizuno, K. Tadanaga, M. Tatsumisago, Electrochim. Acta 50 (2004) 893–897.
[19] Y. Diao, K. Xie, S. Xiong, X. Hong, J. Power Sources 235 (2013) 181–186.
[20] C. Zhang, S. Pang, Q. Kong, Z. Liu, H. Hu, W. Jiang, P. Han, D. Wang, G. Cui, RSC Adv. 3 (2013) 1336–1340.
[21] H. Zhang, X. Yu, P.V. Braun, Nature Nanotech. 6 (2011) 277–281.
[22] J. Chen, L. Yang, S. Fang, S.I. Hirano, K. Tachibana, J. Power Sources 199 (2012) 341–345.
[23] J. Liu, Y. Zhou, J. Wang, Y. Pan, D. Xue, Chem. Commun. 47 (2011) 10380–10382.
[24] Z.W. Seh, W. Li, J.J. Cha, G. Zheng, Y. Yang, M.T. McDowell, P.C. Hsu, Y. Cui, Nat. Commun. 4 (2013) 1331–1336.
[25] W.M. Zhang, J.S. Hu, Y.G. Guo, S.F. Zheng, L.S. Zhong, W.G. Song, L.J. Wan, Adv. Mater. 20 (2008) 1160–1165.
[26] Y. Lei, H. Jia, Z. Zheng, Y. Gao, X. Chen, H. Hou, CrystEngComm 13 (2011) 6212–6217.
[27] A.L. Abdelhady, K. Ramasamy, M.A. Malik, P. O'Brien, S.J. Haigh, J. Raftery, J. Mater. Chem. 21 (2011) 17888–17895.
[28] Y. Cao, X. Li, I.A. Aksay, J. Lemmon, Z. Nie, Z. Yang, J. Liu, Phys. Chem. Chem. Phys. 13 (2011) 7660–7665.
[29] N. Jayaprakash, J. Shen, S.S. Moganty, A. Corona, L.A. Archer, Angew. Chem. Int. Ed. 50 (2011) 5904–5908.

[30] N. Machida, Solid State Ionics 175 (2004) 247–250.
[31] Y. Yu, C.H. Chen, J.L. Shui, S. Xie, Angew. Chem. Int. Ed. 44 (2005) 7085–7089.
[32] R. Xu, I. Belharouak, J.C.M. Li, X. Zhang, I. Bloom, J. Bareño, Adv. Energy Mater. 3 (2013) 833–838.
[33] K. Kumaresan, Y. Mikhaylik, R.E. White, J. Electrochem. Soc. 155 (2008) A576–A582.
[34] S.E. Cheon, S.S. Choi, J.S. Han, Y.S. Choi, B.H. Jung, H.S. Lim, J. Electrochem. Soc. 151 (2004) A2067–A2073.
[35] C. Barchasz, J.C. Leprêtre, F. Alloin, S. Patoux, J. Power Sources 199 (2012) 322–330.
[36] Y.J. Choi, Y.D. Chung, C.Y. Baek, K.W. Kim, H.J. Ahn, J.H. Ahn, J. Power Sources 184 (2008) 548–552.
[37] J.J. Chen, Q. Zhang, Y.N. Shi, L.L. Qin, Y. Cao, M.S. Zheng, Q.F. Dong, Phys. Chem. Chem. Phys. 14 (2012) 5376–5382.
[38] N. Feng, D. Hu, P. Wang, X. Sun, X. Li, D. He, Phys. Chem. Chem. Phys. 15 (2013) 9924–9930.